Ideal Efficiency of Propellers: Theodorsen Revisited

H. S. Ribner*
University of Toronto, Downsview, Ontario, Canada and NASA Langley Research Center, Hampton, Virginia
and
S. P. Foster†
University of Toronto, Downsview, Ontario, Canada

Theodorsen's 1948 analog evaluation of the parameters governing the ideal (friction-free) efficiency of propellers is updated and extended by computer. The results are presented both in his format and in a much more convenient one by Kramer that avoids iteration: curves of power coefficient at constant ideal efficiency are plotted vs propeller advance coefficient. The curves for a wide range of blade numbers are collapsed into just three sets (with some approximation) by use of multiple, shifted (and distorted) abscissae scales. Along with an overview of Theodorsen's theory, analytic asymptotic results at low and high advance coefficients are given. At the low end, the disagreement with actuator disc theory is given support and physical interpretation. At the high end, exact agreement is found with the thrust of a slender twisted delta propeller.

Nomenclature

This listing is not exhaustive: many symbols of local usage in derivations are omitted. The term Trefftz plane refers to an infinite plane normal to the spin axis far behind the propeller where asymptotic conditions are attained in the helicoid wake.

A = area of cross section of one turn of helicoid wake projected on Trefftz plane (πR_∞^2)
B = number of blades
c_s = thrust coefficient [$T/(\frac{1}{2}\rho V^2 \pi R_\infty^2)$]; see Eq. (11)
c_p = power coefficient [$P/(\frac{1}{2}\rho V^3 \pi R_\infty^2)$]; see Eq. (12)
D = propeller diameter (maps into D_∞ at Trefftz plane)
$K(x)$ = nondimensional blade circulation, $K(x) = \Gamma(x)/wL$
L = axial separation of helicoid turns near Trefftz plane [$2\pi(V+W)/\omega B$]
n = propeller revolutions/s ($\omega/2\pi$)
P = propeller power
p = local static pressure; also, propeller pitch
p_0 = ambient static pressure
Q = propeller torque
R = radius of propeller
R_∞ = radius of contracted wake at Trefftz plane ($D_\infty/2$)
r = radial distance from propeller axis
S = area
T = propeller thrust
V = forward speed of propeller
v = disturbance velocity arising from axial speed w of helicoid wake (components v_z, v_r, v_θ)
v_z = axial component of v
$\bar{v}_z(r)$ = axial average of v_z between turns (r, θ fixed)
w = rearward speed of helicoid wake at Trefftz plane
$\bar{w}$ = w/V
x = signifies r/R at propeller, maps into r/R_∞ at Trefftz plane
z = axial distance downstream from propeller plane
$\Gamma(x)$ = circulation distribution; equals jump in Φ across helicoid surface at x
ϵ = "axial loss factor" ($\int v_z^2\, dS/w^2A$ evaluated over Trefftz plane)
η = propeller ideal efficiency (c_s/c_p)
κ = "mass coefficient" ($\int v_z\, dS/wA = \int v^2\, dS/w^2A$ evaluated over Trefftz plane)
λ = advance coefficient based on V and R_∞ ($V/\omega R_\infty = V/\pi n D_\infty = J_\infty/\pi$)
λ_T = Theodorsen's generalized advance coefficient [$(V+w)/\omega R_\infty = (1+\bar{w})\lambda$]
ρ = fluid density
Φ = velocity potential
ω = propeller angular velocity
Ω = angular velocity of helicoid rotation that is kinematically equivalent to axial motion with speed w [Eq. (17)]

Introduction

MODERN computer oriented methods of propeller performance prediction (cf., e.g., Ref. 1) include some of impressive accuracy.[2,3] But for design purposes they lack an important guideline, namely, the optimum or highest efficiency that might be possible for specified operating conditions, neglecting blade profile drag. Determination of this ideal efficiency is the object of the present paper, largely a partial update of the work of Theodorsen.[4-8] (In what follows, we refer, unless specified otherwise, to his summary book, Ref. 8.)

Betz[9] showed that the ideal efficiency is associated with an optimum blade loading that produces a rigidly moving helicoid wake. The theory for this scenario was developed analytically by Goldstein[10] for lightly loaded propellers. This stimulated a host of applications with varying degrees of approximation (e.g., Ref. 11). Particularly noteworthy was a paper in 1938 by Kramer,[12] adapted to heavily loaded propellers by clever approximations. Then, during the forties, the Goldstein approach was generalized by Theodorsen in a rigorous fashion to cover the heavy loading case. The apparent absence of any further development of the subject since then has motivated the present effort.

Theodorsen's theory of propellers consists of two parts. The first and most significant is the development of the optimum blade circulation distribution for maximum efficiency, excluding profile and wave drag. Two key parameters are evaluated therefrom as functions of a generalized advance coefficient; inserted in simple formulas, they yield the "ideal" (friction-free) thrust, power, and associated efficiency. Evaluation is made for various numbers of blades and even for dual rotation.

Received June 28, 1989; revision received March 26, 1990.

*Professor Emeritus, Institute for Aerospace Studies; NASA Distinguished Research Associate. Fellow AIAA.
†Research Associate, Institute for Aerospace Studies.

The second part consists of a formalism for arriving at the geometry of such optimum propellers, allowing now for the profile drag. Although useful for preliminary design, this section is only approximate; it involves the notion (taken from early wing theory) that the flow around each section of the blade is locally two-dimensional. The appropriate local velocity is compounded from the forward velocity, the rotational velocity, and (in a light-loading approximation) one-half the velocity induced at the same fractional radius far back on the axially moving helicoid wake.

The real flow is, of course, three-dimensional; its departure from the assumed flow increases as the blade aspect ratio decreases. There will be an error in predicted performance that is in part a neglect of an induced camber effect: the actual wake induction velocity will vary along the blade chord. Modern computer oriented methods must be employed to obtain the correct three-dimensional flow. These are, for example, panel methods and, for detailed flow between the blades (including shocks), Euler equation solvers on a three-dimensional grid.

In the present paper we deal solely with the first part of Theodorsen's theory, his development of the ideal thrust, power, and efficiency of propellers (restricted in our case to single rotation). We restate key parts of the development but in different terms; this is partly to establish the credibility of the formalism and partly to assist in the interpretation. Then we set up computer methods to generate his blade circulation $K(r/R)$ and the parameters κ and ϵ/κ derived therefrom. This procedure replaces his ingenious electrical analog scheme: measurements on thin plastic helicoid model wakes in a conducting fluid. Further, we adopt a much more convenient format, due to Kramer,[12] for an alternate presentation of the results: for each number of blades, we give curves of power coefficient vs advance ratio, at constant efficiency. Theodorsen's format, on the other hand, is awkward to use: an iteration procedure involving the initially unknown helicoid wake velocity w is required to determine the generalized advance coefficient $(V+w)/\pi nD_\infty$. We have in effect carried out this iteration in preparing the Kramer style curves and some others.

A much fuller treatment of the present subject will be found in the slightly amended MA.Sc. thesis, Ref. 13. It presents, along with other matters, an alternative, greatly expanded overview of Theodorsen's theory, including his methodology for propeller design (omitted from this paper). Curves for a wide range of blade numbers are presented individually, not subjected to an approximate collapse to save space as herein (see abstract). Further, the analysis of the wake contraction is extended to heavy loading (w/V up to 2) with extensive computed charts.

Theodorsen's Formulation

Optimum Circulation $K(x=r/R)$

The blades of a rotating propeller shed trailing vorticity along their helical paths. According to Betz,[9] when the helicoid sheet from each blade moves backward as if rigid, the efficiency for a given power is a maximum. This implies an optimum distribution of circulation $\Gamma(r)$ along the blades. It must be such that the trailing vorticity of magnitude $d\Gamma/dr$ induces just the right motion. Evaluation of this optimum $\Gamma(r)$, and parameters depending on it, is the central task of the theory.

The above applies for lightly loaded propellers. Theodorsen generalized the scenario to heavily loaded propellers. On this view, there is initial distortion near the propeller, but far back the (multiple) helicoid sheet moves rigidly with axial velocity w. (There is also a contraction of the radius R to R_∞, which is normally only a few percent or less, except at small λ.)[8] Whereas the propeller advance coefficient is

$$\lambda_p = V/\omega R \ (= V/\pi nD) \tag{1}$$

the helicoid advance coefficient is

$$\lambda_T = (V+w)/\omega R_\infty \tag{2}$$

The use of Eq. (2) in place of Eq. (1) to apply to the helicoid is one of the chief differences between the formalism of Theodorsen and that of Goldstein and other earlier workers. But, as noted in the Introduction, the price of this generalization is the necessity for iteration to determine the initially unknown w. (In what follows, it will be convenient for computational reasons to approximate λ_p by $\lambda = V/\omega R_\infty$.)

Theodorsen maps the optimum circulation $\Gamma(r/R)$ along the blades into an unaltered circulation $\Gamma(r/R_\infty)$ in the contracted helicoid far wake ($R \to R_\infty$). Note that $\Gamma(r/R_\infty)$ is equivalently the potential jump across the helicoid surface at r; it is, thus, also the potential difference between successive turns at r (of axial separation L). It follows that $\Gamma(r/R_\infty)/L$ is the axial average value of axial velocity, $\bar{v}_z$, at radius r. The average over the whole helicoid cross section and out to $r=\infty$, in ratio to w, is

$$\kappa = \frac{\int \bar{v}_z(x)\,dS}{wA} = \frac{\int_A \Gamma(x)\,dS}{wAL}, \quad x \equiv r/R_\infty, \quad A = \pi R_\infty^2 \tag{3}$$

noting that the axial (or circumferential) average of v_z is zero for $r > R$. (Actually, the axial average in the foregoing is an unnecessary artifice; thus, $\bar{v}_z$ may be replaced by v_z [cf. Eq. (9)].

Since the tangent of the helix angle is $(V+w)/\omega r$, it can be inferred that $L = 2\pi(V+w)/\omega B$, where B is the number of blades. Thus, if we define a nondimensional circulation as

$$K(x) = \Gamma(x)/wL, \qquad L = 2\pi(V+w)/\omega B \tag{4}$$

Eq. (3) may be written as

$$\kappa = 2\int_0^1 K(x)x\,dx \tag{5}$$

Theodorsen calls κ the "mass coefficient" (among other terms).

Thrust, Power, and Efficiency[7]

Theodorsen's basic equations effectively state the steady flow conservation laws for a large control surface enveloping the propeller and its wake. Conservation of momentum and mass lead to thrust as

$$T = \rho\int\left[(V+w)v_z + v_z^2 - \frac{1}{2}v^2\right]dS \tag{6}$$

and conservation of energy and mass lead to power as

$$P = \rho\int(V+w)(Vv_z + v_z^2)\,dS \tag{7}$$

integrated over an infinite plane perpendicular to the wake axis, far back ("Trefftz plane"). From the unsteady Bernoulli equation, the relation

$$p - p_0 = \rho w v_z - \tfrac{1}{2}\rho v^2 \tag{8}$$

has been used in both to express a pressure term in terms of velocity. (The disturbance velocity field of the helicoid moving axially with speed w is a similarly moving pattern; hence, the velocity potential has the form $\Phi = \Phi(z-\omega t, r, \theta)$. This allows the unsteady term in the Bernoulli equation to be written as $\rho\partial\Phi/\partial t = -\rho w\partial\Phi/\partial z$.)

For evaluation of T and P, we require the Trefftz plane integrals of v_z, v^2, and v_z^2. The first, in nondimensional form,

is just the "mass factor" κ, and Theodorsen shows it is equal to the second:

$$\kappa \equiv \int \frac{v_z\, dS}{wA} = \int \frac{v^2\, dS}{w^2 A} \tag{9}$$

The third, in nondimensional form, is

$$\epsilon \equiv \int \frac{v_z^2\, dS}{w^2 A} \tag{10}$$

and is called the "axial loss factor." In terms of these, the nondimensional thrust and power are obtained from Eqs. (6) and (7) as

$$c_s = T/\tfrac{1}{2}\rho V^2 A = 2\kappa\bar{w}\left[1+\bar{w}(\tfrac{1}{2}+\epsilon/\kappa)\right], \quad \bar{w} = w/V \tag{11}$$

$$c_p = P/\tfrac{1}{2}\rho V^3 A = 2\kappa\bar{w}(1+\bar{w})(1+\bar{w}\epsilon/\kappa) \tag{12}$$

The ideal efficiency is then

$$\eta = TV/P = c_s/c_p = \frac{1+\bar{w}(\tfrac{1}{2}+\epsilon/\kappa)}{(1+\bar{w})(1+\bar{w}\epsilon/\kappa)} \tag{13}$$

Mass Factor κ and Loss Factor ϵ

It follows from these equations that κ and ϵ are the key parameters in Theodorsen's theory; if these are known for given operating conditions, the ideal thrust, power, and efficiency are determined. For physical interpretation we recall that κ and ϵ are connected with the flow due to the axial motion of a multiple helicoid of cross section A. This moving helicoid is equivalent dynamically to a cylinder of fluid moving rigidly, without spillage or swirl, of smaller effective area A_{eff}. With respect to axial momentum and also total kinetic energy, the effective area is [cf. Eq. (9)]

$$A_{\text{eff}} = \kappa A \tag{14}$$

With respect to axial kinetic energy, the effective area is [cf. Eq. (10)]

$$A_{\text{eff}} = \epsilon/A \tag{15}$$

The connection between κ and $K(x)$ is given by Eq. (5). Both depend on the number of blades B and the generalized advance coefficient $\lambda_T = (V+w)/\omega R_\infty$. The connection between ϵ and these is

$$\epsilon = \kappa + \tfrac{1}{2}\lambda_T \frac{d\kappa}{d\lambda_T} \tag{16}$$

according to a derivation by Theodorsen. Algorithms for computer evaluation of $K(x)$, κ, and ϵ are given in another section.

Approach to Twisted Delta Results: $\lambda \to \infty$

The helicoid may be regarded equivalently as moving axially with velocity w or rotating with angular velocity Ω. On examining the geometry, the tangent of the helix angle ϕ at $r = R_\infty$ for equivalent w and Ω can be seen to be

$$\tan\phi = \lambda_T = \frac{V+w}{\omega R_\infty} = \frac{V}{(\omega-\Omega)R_\infty} = \frac{p}{2\pi R_\infty} \tag{17}$$

When $\lambda \to \infty$, the pitch $p \to \infty$ likewise, and for two blades ($B=2$) the helix stretches almost into a ribbon of semiwidth R_∞. We may regard the quasiribbon as rotating about its axis with velocity Ω. Theodorsen defined [see Eq. (9)]

$$\text{kinetic energy/unit length} = \kappa^{(B)}(\pi/2)\rho w^2 R_\infty^2 \qquad B \text{ blades} \tag{18}$$

Now the wake of a slender delta propeller of large pitch is likewise a quasiribbon. This two-blade case was analyzed by Ribner[14] who found

$$\text{kinetic energy/unit length} = (\pi/16)\rho\Omega^2 R_\infty^4 \qquad 2 \text{ blades} \tag{19}$$

Equating evaluates Theodorsen's $\kappa^{(B)}$ for $B=2$ as

$$\kappa^{(2)} = \tfrac{1}{8}(\Omega R_\infty/w)^2 = \beta^2/8\lambda^2 \tag{20}$$

The second form results from the equivalence relations [Eq. (17)] and the definition

$$\beta = \frac{V/\omega R_\infty}{p/2\pi R_\infty} = \frac{V/\omega R_\infty}{(V+w)/\omega R_\infty} \tag{21}$$

together with

$$\Omega = \omega(1-\beta) \qquad \text{and} \qquad w = V(1-\beta)/\beta \tag{22}$$

which can be inferred from Eqs. (17) and (21), respectively, after some manipulation. These may be inserted in Theodorsen's expression [Eq. (11)] for the thrust T, rewritten in the form

$$T^{(2)} = \pi R_\infty^2 \rho\kappa^{(2)} V^2 \bar{w} + (\pi/2) R_\infty^2 \rho\kappa^{(2)} V^2 \bar{w}^2 (1 + 2\epsilon^{(2)}/\kappa^{(2)}) \tag{23}$$

to yield (in terms of $D_\infty = 2R_\infty$), with $\epsilon^{(2)}/\kappa^{(2)} \to 0$ as $\lambda \to \infty$

$$T^{(2)} = (\pi/128)\rho\omega^2 D_\infty^4 \beta(1-\beta) + (\pi/256)\rho\omega^2 D_\infty^4 (1-\beta)^2 \tag{24}$$

Equation (24) is precisely the expression obtained by Ribner[14] for the thrust of a slender delta propeller of very large pitch. The first term may be identified with that part of the thrust due to surface pressure and the second term may be identified with the part due to leading-edge suction. [The second term may also be interpreted as $\int (p-p_0)^{dS}$ taken over the Trefftz plane. See Eqs. (8) and (9) herein for the form in Eq. (23) and Appendix C of Ref. 14 for a direct calculation.] Theodorsen's general Eq. (11), it will be recalled, was obtained from the conservation equations applied to a large control surface containing the propeller and its helicoidal wake. *It seems rather remarkable that the equation breaks naturally into two parts, each of which has a precise physical interpretation in the limiting case of a slender twisted delta of large pitch.*

$\lambda \to \infty$: λ Shift for Curve Collapse, All Blade Numbers

Extending the argument from 2 to B blades, for $\lambda \to \infty$, the pitch of the helicoid sheet from each blade is so large it is essentially a rotating ribbon. Ribner showed that the corresponding propeller torque for 2 blades is

$$Q_\infty^{(2)} = (2V/\omega) \times (\text{kinetic energy/unit length})^{(2)} \tag{25}$$

Thus, at constant $\lambda = V/\omega R$, the torque scales with the kinetic energy per unit length. This is true even if the (multiple) ribbon corresponds to B blades rather than Ribner's two. It follows from Theodorsen's definition of κ, Eq. (9), that

$$\kappa^{(B)}/\kappa^{(2)} = Q_\infty^{(B)}/Q_\infty^{(2)} \qquad \lambda \gg 1 \tag{26}$$

From Eqs. (20) and (21), $\kappa^{(2)}$ is evaluated as

$$\kappa^{(2)} = 1/\left[8\lambda^2(1+\bar{w})^2\right] = 1/8\lambda_T^2 \qquad \lambda \gg 1 \tag{27}$$

so that

$$\kappa^{(B)} = 1/\left[8\lambda^2(1+\bar{w})^2\right]\left[Q_\infty^{(B)}/Q_\infty^{(2)}\right] \qquad \lambda \gg 1 \tag{28}$$

Thus, we may define an effective λ as

$$\lambda_{\text{eff}} = \lambda\sqrt{Q_\infty^{(2)}/Q_\infty^{(B)}} \qquad \lambda \gg 1 \tag{29}$$

such that Eq. (28) becomes

$$\kappa^{(B)} = 1\Big/\left[8\lambda_{\text{eff}}^2(1+\bar{w})^2\right] \qquad \lambda \gg 1 \tag{30}$$

which applies for any number of blades B. Thus, the use of λ_{eff} in the place of λ collapses the separate curves of $\kappa^{(B)}$ for all B into a single curve. As derived, this λ shift (in a logarithmic sense) is applicable strictly to $\lambda \gg 1$. However, it effects an approximate collapse when applied over the *whole range* of λ but with increasing error as $\lambda \to 0$. In our calculated results (in Kramer's format only), we have locally adjusted this λ shift to minimize the error.

The torque ratio $Q_\infty^{(2)}/Q_\infty^{(B)}$ has been evaluated by Ribner in another paper[15] and in effect by Kramer.[12] They used a solution by Westwater[16] for the potential flow about a rotating multiblade ribbon. The values of $\sqrt{Q_\infty^{(2)}/Q_\infty^{(B)}}$ are given in Table 1 and compared with an empirical formula $(\frac{1}{2})\sqrt{1+6/B}$ suggested by Kramer for $\lambda_{\text{eff}}/\lambda$ at large λ.

Collected Asymptotic Results

In the last section, we evaluated κ in terms of λ as $\lambda \to \infty$; it suffices to know that the corresponding value of $\epsilon/\kappa \to 0$, according to Eq. (16). On the other hand, for $\lambda \to 0$, Theodorsen shows that both κ and $\epsilon/\kappa \to 1$. From these results and the general equations for efficiency η, and thrust coefficient c_s, respectively, the asymptotic results follow in sequence. They are as follows.

Arbitrary Number of Blades, B

$\lambda = 0$		$\lambda \to \infty$	
$\kappa = 1$	(31a)	$\kappa = Q_\infty^{(B)}/Q_\infty^{(2)}\left[1/8\lambda^2(1+\bar{w})^2\right] \to 0$	(31b)
$\epsilon/\kappa = 1$	(32a)	$\epsilon/\kappa \to 0$	(32b)
$\eta = \left[1+(3/2)\bar{w}\right]/(1+\bar{w})^2$	(33a)	$\eta = \left[1+(1/2)\bar{w}\right]\Big/(1+\bar{w})$	(33b)
$\bar{w} = \dfrac{-(2\eta-3/2)\pm\sqrt{(2\eta-3/2)^2+4\eta(1-\eta)}}{2\eta}$	(34a)	$\bar{w} = 2(1-\eta)/2\eta - 1$	(34b)
$c_s = 2\bar{w} + 3\bar{w}^2$	(35a)	$c_s = \dfrac{Q_\infty^{(B)}}{Q_\infty^{(2)}}\dfrac{\bar{w}(1+\frac{1}{2}\bar{w})}{4\lambda^2(1+\bar{w})^2}$	(35b)
or			
$c_s = 2\bar{w}(1+\bar{w})^2\eta$	(36a)	$c_s = \dfrac{Q_\infty^{(B)}}{Q_\infty^{(2)}}\dfrac{\eta(1-\eta)}{2\lambda^2}$	(36b)

where

$$\bar{w} = \frac{w}{V};\quad \eta = \frac{c_s}{c_p};\quad c_s = \frac{\text{thrust}}{\frac{1}{2}\rho V^2\pi R_\infty^2};\quad c_p = \frac{\text{power}}{\frac{1}{2}\rho V^3\pi R_\infty^2} \tag{37}$$

(The reciprocal square root of the torque ratio for $Q_\infty^{(B)}/Q_\infty^{(2)}$, $\lambda \to \infty$, was evaluated numerically in Table 1 of the last section for a range of blade numbers B.)

Infinite Number of Blades, $B = \infty$

For $B \to \infty$, the separation of turns in the multiple helicoid (one from each blade) approaches zero for arbitrary advance λ (as it does for $\lambda \to 0$ and arbitrary B). This simplification allows closed form evaluation of the parameters. Theodorsen gives

$$K(x;\lambda_T) = x^2/(\lambda_T^2 + x^2), \qquad x \equiv r/R_\infty \tag{38}$$

$$\kappa(\lambda_T) = 2\int_0^1 Kx\,dx, \qquad \lambda_T \equiv \lambda(1+\bar{w}) \tag{39}$$

$$= 1 - \lambda_T^2\,\ell n(1+\lambda_T^{-2}) \tag{40}$$

$$\epsilon(\lambda_T) = 1 + \lambda_T^2/(1+\lambda_T^2) - 2\lambda_T^2\,\ell n(1+\lambda_T^{-2}) \tag{41}$$

Numerical Algorithms

Helical Vortex Strength Dictated by Rigid Motion

We require to determine the radial distribution of circulation $\Gamma(x = r/R_\infty)$ far back in the multiple helicoid propeller wake (i.e., in the Trefftz plane). For the computer, we model this (for each of the B helicoid sheets, one from each blade) as a summation of helical vortices $\gamma_j = (-d\Gamma_j/dx)\Delta x$ separated radially by Δx. The following development leads to an algorithm for the determination of the γ_j.

Let P_i be any point on an individual helicoid surface, with Cartesian coordinates ζ_i^α, $\alpha = 1,2,3$; ζ_i^1 is in the radial direction, ζ_i^2 is in the circumferential direction, and ζ_i^3 is along the propeller/helicoid axis directed downstream, with $\zeta_i^3 = 0$ designating the choice of Trefftz plane. The local axial surface displacement velocity is w, the local velocity induced thereby is $v_i = v_i^\alpha$, and the local surface normal (downstream side) is $N_i = N_i^\alpha$. Then the boundary condition of tangential flow requires that

$$v_i \cdot N_i = w\cos\varphi_i = \sum_\alpha v_i^\alpha N_i^\alpha;\ \alpha = 1,2,3 \tag{42}$$

where

$$N_i^1 = 0,\ N_i^2 = -\sin\varphi_i,\ N_i^3 = \cos\varphi_i;\ \varphi_i = \tan^{-1}[(V+w)/\omega r_i] \tag{43}$$

and φ_i is the local helix angle. Betz[9] condition for rigid motion of the helicoid (applicable only well behind the propeller) requires that all surface points move with the same speed: w is a constant. Now v_i^α is induced by the helical vortices γ_j, representing the entire multiple helicoid. We express it as w times a nondimensional summation

$$v_i^\alpha = \sum_j v_{ij}^\alpha = w\sum_j c_{ij}^\alpha\hat{\gamma}_j, \qquad \hat{\gamma}_j = \gamma_j/wL \tag{44}$$

where the c_{ij}^α are vortex influence coefficients to be derived. Insertion into Eq. (42) gives

$$\sum_\alpha\sum_j c_{ij}^\alpha N_i^\alpha\hat{\gamma}_j = \cos\phi_i \tag{45}$$

Interchange the order of α and j summations and define

$$F_{ij} = \sum_\alpha c_{ij}^\alpha N_i^\alpha \tag{46}$$

Table 1 Values of $\lambda_{\text{eff}}/\lambda$ [Eq. (29)]

B	1	2	3	4	6	8	∞
$\sqrt{Q_\infty^{(2)}/Q_\infty^{(B)}}$	1.333	1.000	0.860	[a]0.785	0.702	0.655	0.500
$(\frac{1}{2})\sqrt{1+6/B}$	1.323	1.000	0.866	0.791	0.707	0.661	0.500

[a] $\pi/4$

giving finally

$$\sum_j F_{ij}\hat{\gamma}_j = \cos\phi_i, \qquad j = 1 \text{ to } M;\ i = 1 \text{ to } M-1; \quad (47)$$

M = number of vortices per blade

as the system of equations to be solved for the unknown nondimensional helical vortex strength $\hat{\gamma}_i$. Herein, F_{ij} is a matrix of scalar influence coefficients; it is obtained from the vector influence coefficients c_{ij}^{α} (derived below) as the dot product with N_i^{α}, Eq. (46). The additional condition of vortex continuity appended to Eq. (47) results in a linear system of rank M.

The influence coefficient c_{ij}^{α} times $\hat{\gamma}_j$ expresses the velocity, in nondimensional form, induced at point P_i by the system of vortices of strength γ_j at a particular radius r_j from all the blades. The Biot-Savart law expresses that velocity in dimensional form as

$$v_{ij}^{\alpha} = wc_{ij}^{\alpha}\hat{\gamma}_j = \frac{\gamma_j}{4\pi}\left(\sum_{k=1}^{B}\int_{\Lambda_k}\frac{\tilde{r}x\tilde{dl}}{|\tilde{r}|^3}\right)^{\alpha} \quad (48)$$

where $\tilde{r}$ is the vector from point P_i to a point on the helical vortex γ_j to point P_i, Λ_k is an infinite helical vortex filament of radius r_j from the kth propeller blade, and $(\ )^{\alpha}$ represents the α-component of the enclosed vector [cf. Eq. (42) and paragraph above]. The specified point on the jth helical vortex is $(\xi_j^1,\xi_j^2,\xi_j^3)$ in Cartesian coordinates; the connection to cylindrical coordinates (r_j,θ) is

$$\xi_j^1 = r_j\cos(\theta+\Psi_k) \qquad \Psi_k = 2\pi(k-1)/B$$

$$\xi_j^2 = r_j\sin(\theta+\Psi_k)$$

$$\xi_j^3 = \lambda_T R_{\infty}\theta = \frac{\theta}{2\pi}p \quad (=0 \text{ at Trefftz plane}) \quad (49)$$

where ξ_j^3 is along the helix axis, and B is the number of blades. Let P_i have coordinates $(\zeta_i^1,\zeta_i^2,\zeta_i^3)$, whence $\tilde{r} = (\xi_j^1 - \zeta_i^1, \xi_j^2 - \zeta_i^2, \xi_j^3 - \zeta_i^3)$, which is expanded below in Eq. (53).

With use of Eqs. (44) and (49), Eq. (48) yields

$$c_{ij}^1 = \int_{-\infty}^{\infty}\frac{\lambda_T^2}{2B}\sum_{k=1}^{B}\frac{(r_j/R_\infty)\sin(\theta+\Psi_k) - (\zeta_i^2/R_\infty) - (r_j/R_\infty)\left[\theta - \zeta_i^3/(R_\infty\lambda_T)\right]\cos(\theta+\Psi_k)}{|\tilde{r}/R_\infty|^3}\,d\theta = 0 \quad (50)$$

$$c_{ij}^2 = \int_0^{\infty} -\frac{\lambda_T^2}{B}\sum_{k=1}^{B}\frac{(r_j/R_\infty)\cos(\theta+\Psi_k) - (\zeta_i^1/R_\infty) + (r_j/R_\infty)\left[\theta - \zeta_i^3/(R_\infty\lambda_T)\right]\sin(\theta+\Psi_k)}{|\tilde{r}/R_\infty|^3}\,d\theta \quad (51)$$

$$c_{ij}^3 = \int_0^{\infty}\frac{r_j\lambda_T}{R_\infty B}\sum_{k=1}^{B}\frac{(r_j/R_\infty) - (\zeta_i^1/R_\infty)\cos(\theta+\Psi_k) - (\zeta_i^2/R_\infty)\sin(\theta+\Psi_k)}{|\tilde{r}/R_\infty|^3}\,d\theta \quad (52)$$

where

$$\left|\frac{\tilde{r}}{R_\infty}\right|^3 = \left[\left(\frac{r_j}{R_\infty}\right)^2 - 2\left(\frac{r_j}{R_\infty}\right)\left\{\frac{\zeta_i^1}{R_\infty}\cos(\theta+\Psi_k) + \frac{\zeta_i^2}{R_\infty}\sin(\theta+\Psi_k)\right\} + \left(\frac{\zeta_i^1}{R_\infty}\right)^2 + \left(\frac{\zeta_i^2}{R_\infty}\right)^2 + \left(\lambda_T\theta - \frac{\zeta_i^3}{R_\infty}\right)^2\right]^{3/2} \quad (53)$$

and the skew symmetry in $\pm\theta$ has been invoked in obtaining zero for c_{ij}^1 and $\int_{-\infty}^{\infty} = 2\int_0^{\infty}$ for c_{ij}^2 and c_{ij}^3. For computation, we may specify $\zeta_i^3 = 0$ without loss of generality: all radial lines in a helicoid are equivalent.

These influence coefficients pose special problems for computer evaluation: 1) the upper limit is infinite, and 2) the number of function evaluations varies as the square of the number of helical vortices. Regarding problem 1, the rapid decay of $|r/R\infty|^{-3}$ with ζ_i^3 permits a truncation approximation scheme: the direct integration is stopped at $\xi_j^3 = 5D_\infty$; further downstream to final truncation at $\xi_j^3 = 15D_\infty$, the helix is approximated as a stack of ring vortices plus an outer sheath of axial vorticity. Regarding problem 2, an efficient procedure is as follows: computations of, e.g., κ are made with $M = 25$, 50, and 100 helical vortices and extrapolated to $M = \infty$ (continuous vortex sheet). A substantial number of check calculations have been made[13] to assess the accuracy of these approximations.

Evaluation of $K(x)$, κ, and ϵ

The γ_i defined as $(-d\Gamma_i/dx)\Delta x$ are effectively just the steps in a staircase approximation to the blade circulation $\Gamma(x)$. The $\hat{\gamma}_i$ form a corresponding staircase approximation to the nondimensional form $K(x)$. For evaluation of the mass factor

$$\kappa = 2\int_0^1 xK(x)\,dx$$

it was convenient to use approximations to $K(x)$ given by the upper and lower bounds of the staircase, to perform two integrations, and to average the results. However, in the procedure the "upper bound," which should be zero at $x = 0$ and $x = 1$, is automatically one "step" height. The error in the asymptotic value of κ as obtained in this way as the number of steps tends to infinity (and hence their heights tend to zero) should be negligible. Some numerical tests have been made that confirm this.

Evaluation of c_s and c_p for B Blades

Equations (11-13) show that thrust, power, and ideal efficiency, c_s, c_p, and η, depend on $\bar{w}$ and on κ and ϵ/κ. The last two are functions of $\lambda_T = \lambda(1+\bar{w})$ (and depend also on B). Thus, when we specify λ and η, $\bar{w}$ is initially unknown. But with λ and η specified, Eq. (13) for η can be solved for the unknown $\bar{w}$.

For each specification, the solution for $\bar{w}$ is carried out numerically by the method of regula-falsi. The required values of κ and ϵ/κ are evaluated at the correct $\lambda_T = \lambda(1+\bar{w})$ with a free variable, by interpolation of a set of previously computed data, $\{\kappa(\lambda_{Ti}),\ 1 \le i \le m\}$. The procedure uses a cubic spline fit to the data, using free end boundary conditions. Specifically, the coefficients β are evaluated in

$$S_i(\lambda_T) = \beta_i^{(0)} + \beta_i^{(1)}(\lambda_T - \lambda_{Ti}) + \beta_i^{(2)}(\lambda_T - \lambda_{Ti})^2 + \beta_i^{(3)}(\lambda_T - \lambda_{Ti})^3, \qquad \lambda_{Ti} \le \lambda_T \le \lambda_{Ti+1} \quad (54)$$

with

$$\kappa(\lambda_T) \approx S_i(\lambda_T) \quad (55)$$

$$\epsilon/\kappa(\lambda_T) \approx 1 + \frac{1}{2}\frac{\lambda_T}{S_i(\lambda_T)}\frac{dS_i(\lambda_T)}{d\lambda_T} \quad (56)$$

Once $\bar{w}$ is determined numerically by the above procedure, the cubic spline interpolation yields numerical values of κ and ϵ/κ; these in turn lead, by substitution into Eqs. (11) and (12), to the required values of $c_s(\lambda;\eta)$ and $c_p(\lambda;\eta)$.

Slipstream Contraction

Theodorsen[8] devotes a chapter to the estimation of the helicoid wake contraction from R at the propeller to R_∞ far back. He incorporates ΔR_∞ into a parameter $Y = Y(\lambda_T;B)$ in the form

$$\Delta R_\infty/R = 2\bar{w}Y, \qquad \Delta R_\infty = R - R_\infty \tag{57}$$

In the derivation of Y, he uses the light loading approximation $c_s/\kappa = 2\bar{w}$ and others. Consistently, we may use another light loading approximation,[12] efficiency $\eta = 1/[1+(\frac{1}{2})\bar{w}]$. This allows Eq. (57) to be rewritten in the form

$$\Delta R_\infty/R = 4Y(1-\eta)/\eta, \qquad \eta \to 1.0(\bar{w}\to 0) \tag{58}$$

We may incorporate into Eq. (58) a first approximation to Theodorsen's Fig. 29 for Y vs λ_T (plus the $\bar{w}=0.01$ curve of Foster's[13] Fig. 53: see below) as

$$\Delta R_\infty/R = 0.5e^{-b\lambda_T}(1-\eta)/\eta, \qquad \eta \to 1.0(\bar{w}\to 0) \tag{59}$$

with $b = 4.05, 2.52, 1.43, 0.98$ for $B = 2, 4, 10, \infty$. Equation (59) will serve for the rough estimation of the correction from R to R_∞ for the cited values of B in cases of high efficiency only.

For a more comprehensive and accurate treatment (and other values of B), the reader is directed to Ref. 13. In this later effort, Theodorsen's "empirical" method for deriving Y is reworked to allow for large values of $\bar{w}$: the individual curves $Y = Y(\lambda_T)$ of his Fig. 29 for each B are generalized into families $\hat{Y} = \hat{Y}(\lambda_T;\bar{w})$. The effect is to reduce Y by four-fold or more when $\bar{w}$ is increased from 0.01 to 2.

The contraction $\Delta R_\infty/R$ is clearly the greatest by far at $\lambda_T = 0$; it agrees there with the result of actuator disc theory, $(\Delta R_\infty/R)_0 = \bar{w}/4$. The quasiexponential reduction in the contraction for finite λ_T is evidently due to the tip effect: the flow spillage around the edges of the helicoid.

Results and Discussion

All the results that follow are referenced to the geometry of the helicoid wake, or "slipstream," far behind the propeller ($z = \infty$); thus, the propeller radius R is replaced by the asymptotic slipstream radius R_∞ (e.g., in the definition $c_p = \text{power}/\frac{1}{2}\rho V^3 \pi R_\infty^2$). For advance coefficient $\lambda = V/\omega R_\infty$ above about 0.5, and conditions of light loading (high efficiency, η), the contraction $(R - R_\infty)$ will be but a few percent, and R_∞ may be approximated as R. For a more quantitative estimate see the previous section, [Eq. (59)], and, for still more accuracy, Ref. 13, especially for cases of heavy loading.

Central to Theodorsen's method[8] are the mass factor κ and the axial energy loss factor ϵ. The ideal thrust, power, and efficiency of the propeller are given as functions [Eqs. (11–13)] of these, the forward velocity V, and the helicoid wake velocity w. In turn, κ is related to the optimum circulation distribution $K(x \equiv r/R_\infty)$.

Figure 1 gives a family of curves of κ vs λ_T for various numbers of blades: $B = 2, 3, 4, 6, 10, 12, \infty$. The generalized advance coefficient $\lambda_T = (V+w)/\omega R_\infty$ therein is seen to be a modification of the more conventional advance coefficient $\lambda = V/\omega R_\infty$. The use of λ_T collapses the curves for all values of the wake velocity w; however, the price is an iteration procedure to determine the initially unknown w. Figure 2 gives corresponding curves of ϵ/κ vs λ_T.

The mass factor κ is the integral of the optimum circulation $K(x \equiv r/R_\infty)$, weighted by $2x$, over the propeller radius. For a two-blade propeller, Fig. 3 presents curves of K vs x for $\lambda_T = 0.1$, 0.25, 0.5, and 1.0. For $\lambda_T = 0.1$ and 0.25, values calculated by Goldstein[6] are superimposed. And for $\lambda_T = 0.5$ and 1.0, values calculated by Kramer[12] are plotted, following

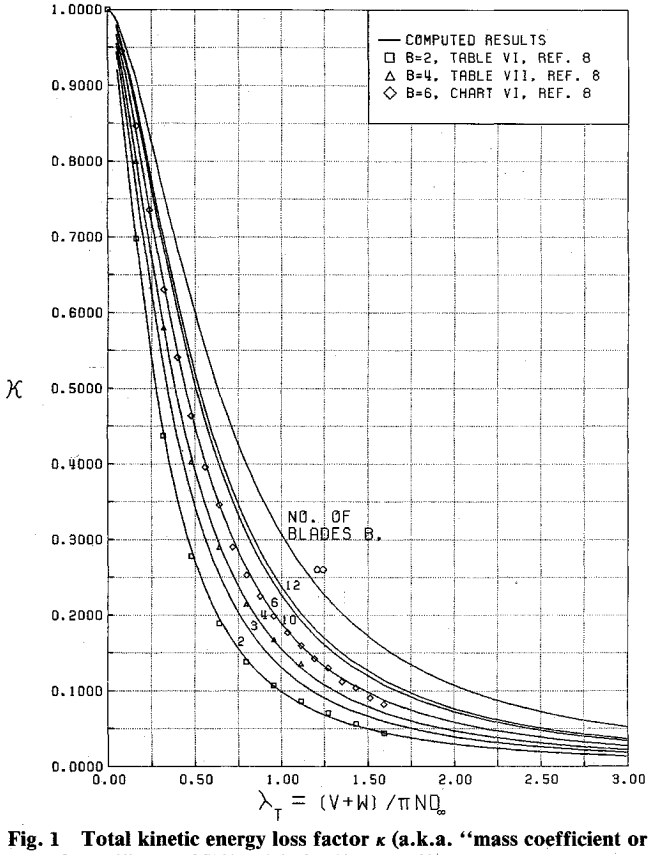

Fig. 1 Total kinetic energy loss factor κ (a.k.a. "mass coefficient or mass factor"), $w \simeq 2V(1-\eta)/\eta$ for light loading.

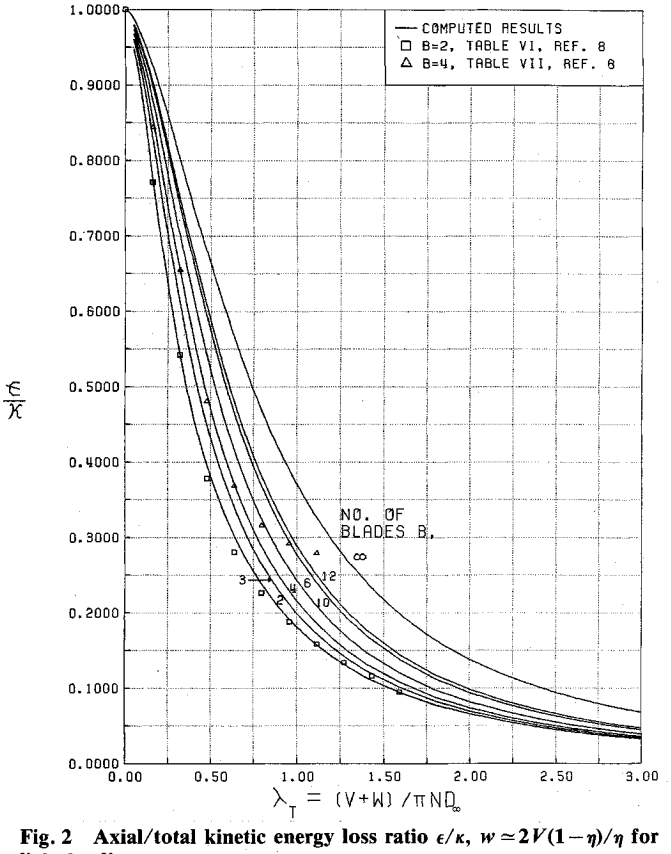

Fig. 2 Axial/total kinetic energy loss ratio ϵ/κ, $w \simeq 2V(1-\eta)/\eta$ for light loading.

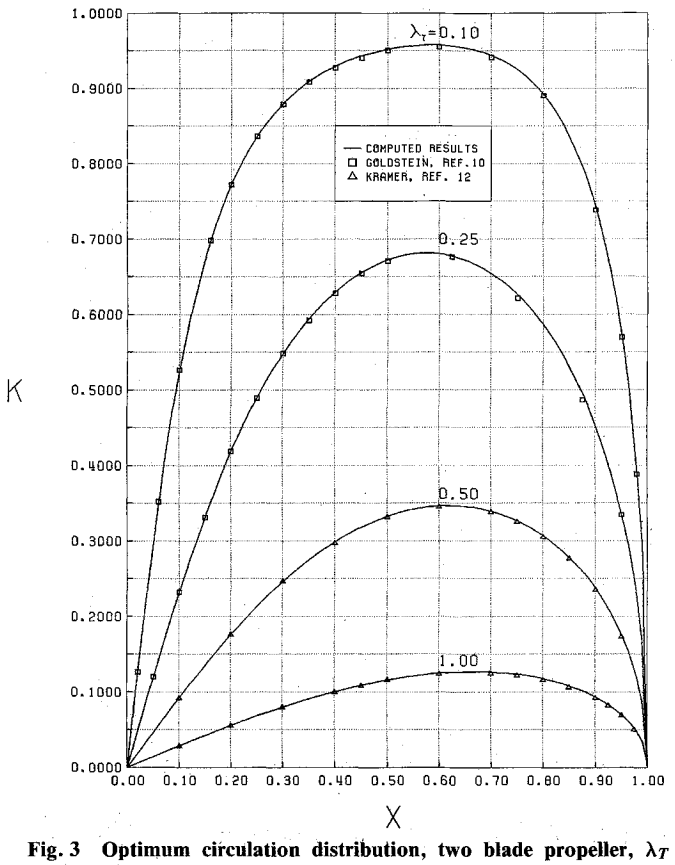

Fig. 3 Optimum circulation distribution, two blade propeller, $\lambda_T = (V+w)/\pi nD$.

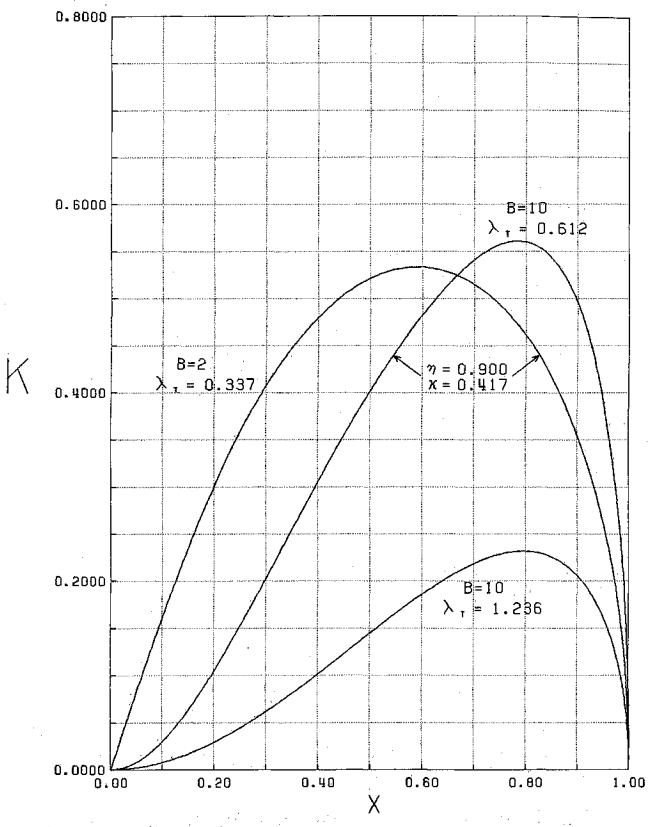

Fig. 4 Optimum circulation distributions. Top two curves (2 blades and 10 blades, respectively) correspond to same efficiency, $\lambda_T = (V+w)/\pi nD$.

Theodorsen in identifying Kramer's $\lambda_i = \lambda/\eta$ with λ_T. Agreement is consistently very close. But it must be noted that λ_i is only an approximation to λ_T.

On Fig. 4, the upper two curves of $K(x)$, one for $B=2$ blades at $\lambda_T = 0.337$ and the other for $B=10$ blades at $\lambda_T = 0.612$, have almost the same area integral when weighted by $2x$. Thus, the values of mass factor κ are virtually the same ($\kappa = 0.417$), as are the efficiencies ($\eta_i = 0.90$). It is in this sense that the respective values of λ_T are "equivalent" for 2 blades and 10 blades. The lower curve, for $B=10$, shows $K(x)$ for a higher advance ratio, $\lambda_T = 1.236$. It is evident from the figure that increasing the number of blades moves the optimum circulation peak toward the blade tips. (Figure 6 of Kramer[12] shows that the peak moves to the very tips for an infinite number of blades.)

Our curves of $K(x)$ closely resemble those of Theodorsen for comparable cases. In order to conserve space, the presentation herein has been limited to Figs. 3 and 4. As a further justification for this, it is observed that propellers are very forgiving for departures from this optimum distribution: the experimental envelope of peak efficiency generally shows a very broad flat maximum in the neighborhood of the design twist distribution (i.e., near the design blade setting).

Figure 5 gives curves of propeller power coefficient $c_p = P/(\frac{1}{2}\rho V^3 \pi R_\infty^2)$ vs advance ratio $\lambda = V/\omega R_\infty$ for various constant ideal efficiencies η; Fig. 5a covers the range $\eta = 0.99$ to 0.85, Fig. 5b the range $\eta = 0.85^*$ to 0.70, and Fig. 5c the range $\eta = 0.70^*$ to 0.50. (Note that the ranges overlap, the repeated values being denoted by asterisks: the curves $\eta = 0.85^*$ and 0.85 differ, but are comparably accurate; the curve $\eta = 70^*$ is less accurate than the curve $\eta = 70$ and should be used for interpolation only. The reasons are elaborated below.) In these figures, the curves for a series of blade numbers 2, 3, 4, 5, 6, 8, 10, 12, ∞ are effectively collapsed into a single curve for each η by use of multiple λ scales. These are slightly distorted logarithmic scales shifted with respect to one another. The concept underlying this useful space-saving scheme, adapted from Kramer,[12] is discussed just after Fig. 6. For more accurate values, the reader is referred to Ref. 13, where the individual uncollapsed curves are presented.

For Fig. 5a, the multiple abscissae scales for $B \neq 2$ were chosen by computer for exact agreement of c_p values with those for $B=2$ at $\eta = \eta_c = 0.92$ (not plotted); for Fig. 5b, at $\eta_c = 0.78$ (not plotted); and for Fig. 5c, at $\eta_c = 0.55$. Thus, the curve collapse is exact only at these respective values of η_c. It follows that the top and bottom curves of Figs. 5a, 5b, and 5c are most in error for $B \neq 2$, since the values of η_c are intermediate. Moreover, the error increases with increasing numbers of blades B. Spot checks were made for $B=8$: the largest error (in c_p) in Fig. 5a was 1.9% on the $\eta = 0.85$ curve at $\lambda = 1.0$; in Fig. 5b it was 2.5% on the $\eta = 0.70$ curve at $\lambda = 1.0$; and in Fig. 5c it was -2.5% on the $\eta = 0.60$ curve at $\lambda = 0.5$. (A larger value -5.6% on the $\eta = 0.70^*$ is irrelevant, since the more accurate curve $\zeta = 0.70$ in Fig. 5b is available; see previous paragraph.)

In order to conserve space, curves of thrust coefficient $c_s = T/\frac{1}{2}\pi V^2 \pi R_\infty^2$ are omitted: the value is readily obtained as ηc_p. Curves of $c_s(\lambda;\eta;B)$ are, however, given in the fuller Ref. 13.

Kramer's approximate predictions[12] of $c_p(\lambda;\eta)$ have been briefly compared with the present results: some thirty spot checks of his Fig. 14 vs our Fig. 5. The errors seem to range from within a few percent to -8% or so in the range of $\eta = 0.99$ to 0.60, and increase to order -20% at $\eta = 0.50$.

Figure 6 shows, for $\lambda = 1$, the variation of ideal efficiency η with power loading c_p for blade numbers $B = 2, 3, 4, 5, 6, 8, 10, 12$, and ∞ (see also Ref. 17 for a similar figure). It displays very graphically the progressive loss in efficiency as the blade number B is reduced. This is the well-known blade tip loss effect. It is loosely ascribed to the "wasted" kinetic energy of the flow induced outside the helicoidal wake as it moves backward. For large B (small tip loss), the turns of the helicoid are

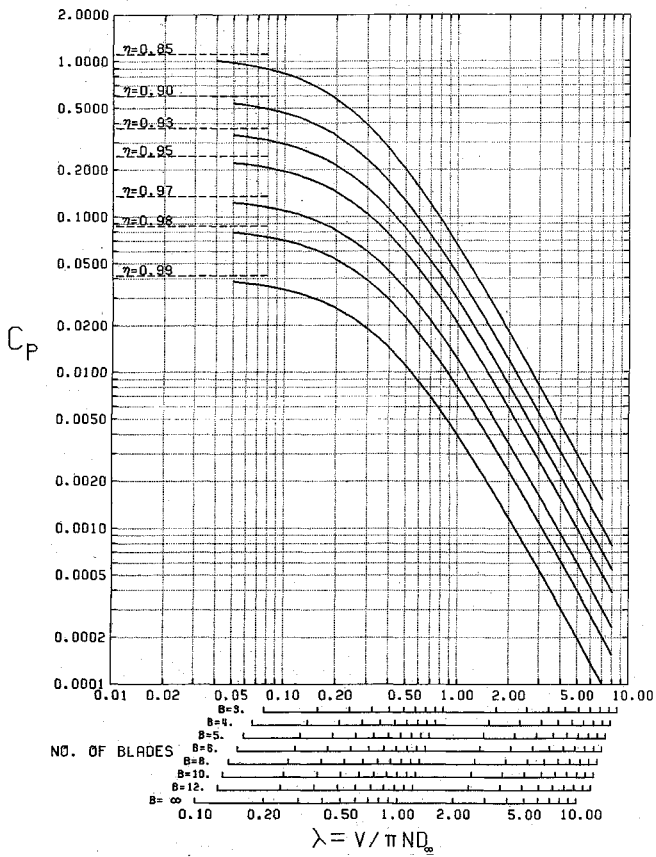

Fig. 5a Power coefficient c_p at constant efficiency η, $0.99 > \eta > 0.85$.

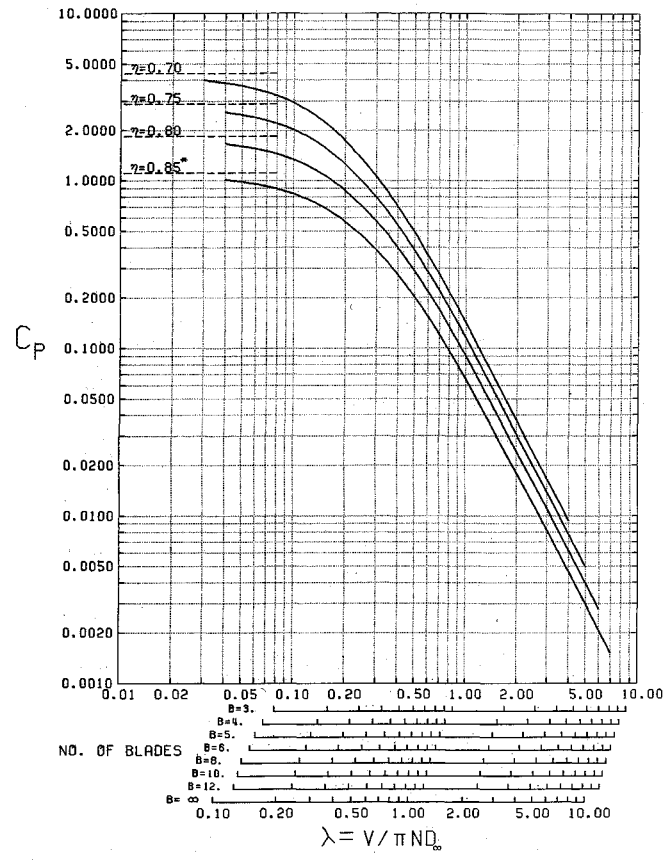

Fig. 5b Power coefficient c_p at constant efficiency η, $0.85^* > \eta > 0.70$.

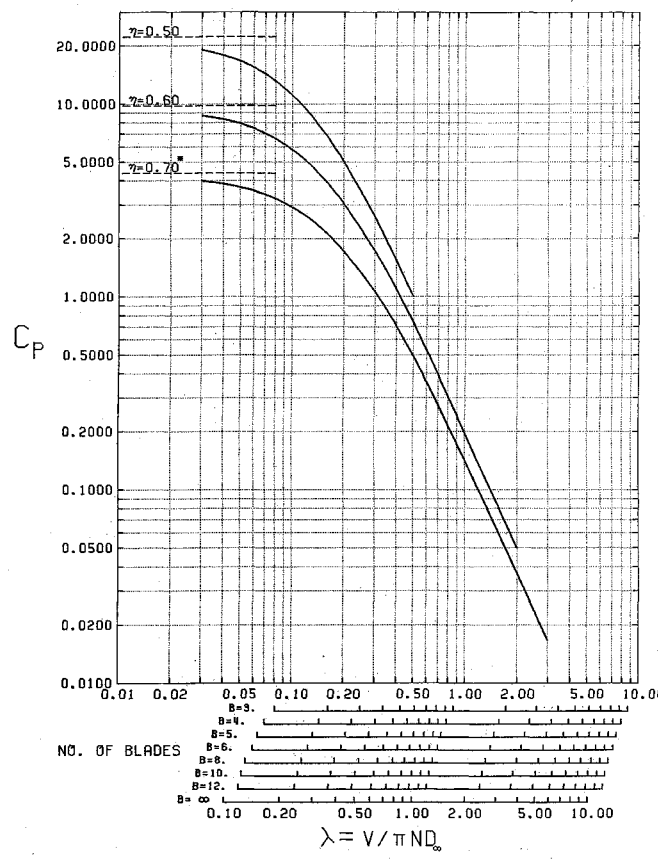

Fig. 5c Power coefficient c_p at constant efficiency η, $0.70^* > \eta > 0.50$.

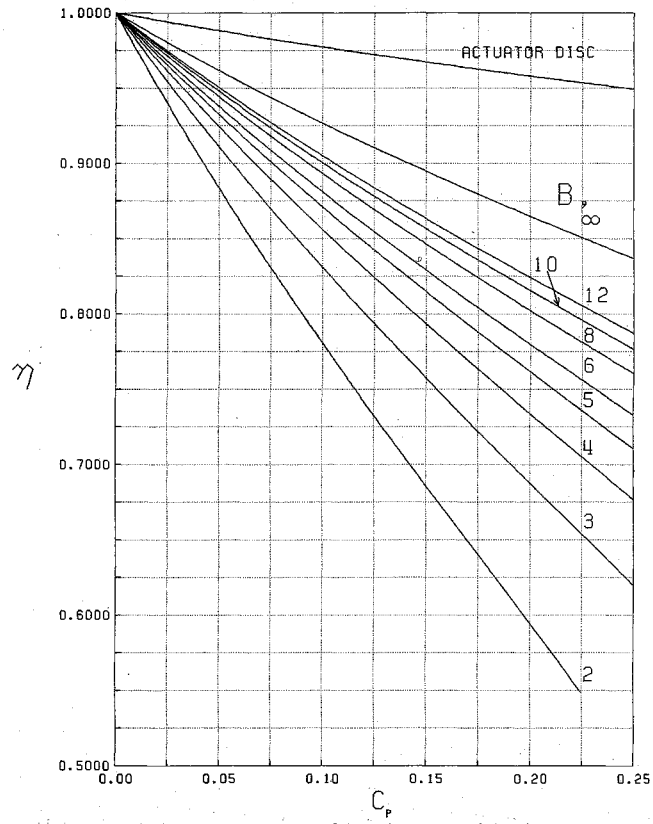

Fig. 6 Ideal efficiency η vs power coefficient c_p at constant advance coefficient, $V/\pi nD_\infty = 1.00$; various numbers of blades B.

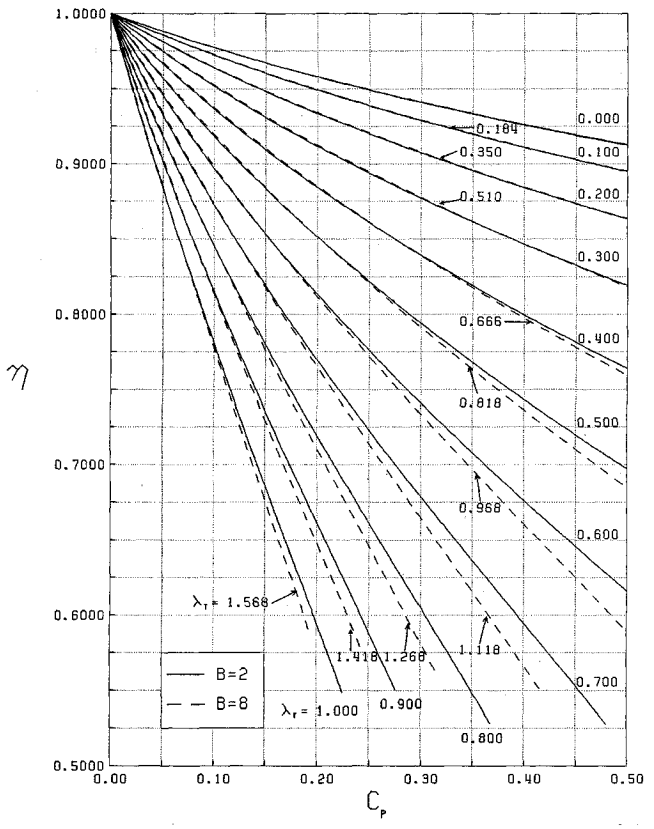

Fig. 7 Ideal efficiency η vs power coefficient c_p for 2 blade and 8 blade propellers at "corresponding" advance coefficients, λ and λ^*, respectively.

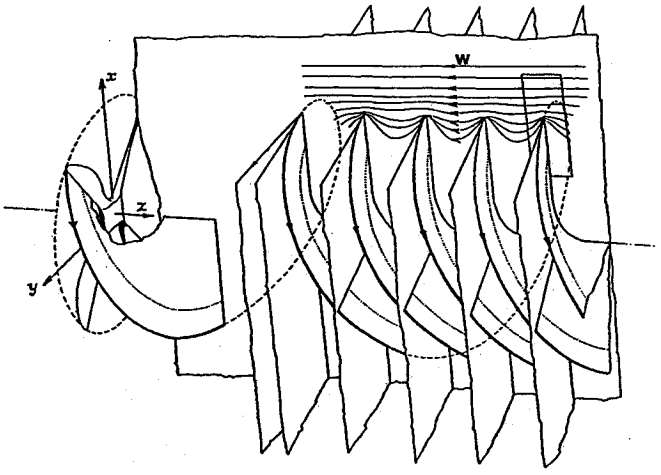

Fig. 8 Relative flow past propeller helicoid wake (in wake-fixed reference frame). Adapted from Fig. 3 of Ref. 18. Pressure gradient associated with flow curvature supports pressure elevation $\frac{1}{2}\rho w^2$ between turns. The tangent planes at the edges are to be ignored.

closely spaced and the flow spillage around the edges is small; for small B (large tip loss), the turns are widely spaced and the spillage is large.

The efficiency for $B = \infty$ (essentially zero tip loss) is seen to lie well below the prediction of the actuator disc model. The loss is attributed to the slipstream swirl of the single rotation propeller, along with other features, that are not accounted for in actuator disc theory.

The significant feature governing tip loss is not the helicoid turn spacing "a" (normal to the turn) per se, but rather its ratio to some other length parameter. Kramer[12] suggests, in effect, that tip loss—hence efficiency—is constant if the parameter $a/\pi R$, which equals $2\lambda/(B\sqrt{1+\lambda^2})$, is constant. This is grossly off the mark quantitatively, but it did lead him to the useful notion of "equivalent" values of λ for different B that would yield the same efficiency. This same concept has been exploited herein in Figs. 5a, 5b, and 5c to collapse the curves for various numbers of blades.

Another application of the λ-equivalence idea is demonstrated in Fig. 7. Compared with Fig. 6, the roles of blade number B and advance ratio λ are interchanged. The solid lines are plots of efficiency η vs power loading for $B = 2$ blades only, but for differing values of λ, namely 0, 0.1, 0.2,... 1.0. The dashed lines are similar plots for $B = 8$ blades, but for respectively "equivalent" values of λ, namely 0, 0.184, 0.345, 0.510, 0.666, 0.818, 0.968, 1.118, 1.268, 1.418, and 1.568. The "equivalence" was effectively chosen to provide a match for efficiencies η above 0.90. However, it is seen that the match is far more extensive.

Concluding Remarks

The striking match of the two sets of curves in Fig. 7—one for two blades and the other for eight blades—demonstrates a tradeoff between number of blades and advance ratio for the same ideal efficiency. For example, a two-blade propeller operating at $\lambda = 0.60$ will behave very similarly to an eight-blade propeller operating at $\lambda = 0.97$: their curves of efficiency vs power loading will virtually coincide at the higher efficiencies.

As a practical matter, of course, the illustrated B vs λ tradeoff for constant ideal efficiency may be subject to prohibitive constraints. In particular, a high flight speed will not permit a design value of $\lambda = V/\omega R_\infty$ much below 1, for to do so would incur resultant tip speeds well into the supersonic with excessive wave drag, noise, and blade stress.

The topmost curve of ideal efficiency η vs c_p in Fig. 7 is a superposition of two: one is the prediction of actuator disc theory (ADT); the other is the asymptotic result of Theodorsen's theory as $\lambda \to 0$. They are indistinguishable on the graph, but the Theodorsen efficiency is in fact slightly lower: from agreement at $c_p = 0$ it is down 0.04% at $c_p = 0.5$ and 0.76% at $c_p = 5$.

In practical terms, the predictions of efficiency are virtually the same. However, the fact of the very small difference supports Theodorsen's assertion that ADT "is not a true limit case for the propeller [as $\lambda \to 0$]." The Theodorsen theory has a pressure term, lacking from ADT, namely, $\int(p - p_0)\, dS$ taken over the Trefftz plane; this accounts for the cited very slight loss in efficiency compared with ADT for $\lambda \to 0$. In this limit, the pressure within the slipstream (helicoid) is predicted to be higher by an amount $p - p_0 = \frac{1}{2}\rho w^2$ than the ambient value p_0 outside. This enhances both the thrust and power consumed at constant w, the latter very slightly more for a minute reduction in efficiency.

We suggest a physical interpretation of the pressure rise Δp in terms of the external flow past the helicoid moving axially with speed w. For $\lambda \to 0$, the turns are closely packed, but separated by a nonvanishing distance L; this harrow-like edge configuration differs from the smooth contour in the actuator disc model. The flow curves in and out of the interstices between the turns (see Fig. 8, adapted from Ref. 18). As the pressure falls from $p = p_0 + (\frac{1}{2})\rho w^2$ in the interior to p_0 outside over a distance of roughly L, the negative pressure gradient is compatible with the local flow curvature, convex outward. As an alternate, compatible point of view, the $\frac{1}{2}\rho w^2$ elevation is the stagnation pressure of the velocity w, which is brought to zero (asymptotically with decreasing r) between the turns.

The pressure term $\int(p - p_0)\, dS$ is extremely important at very high advance coefficients. For large λ, the propeller wake is almost a rotating ribbon, and its motion produces a nonzero integrated pressure rise. As evaluated independently[14] in this asymptotic case, it accounts for the thrust component of the leading-edge suction for a slender twisted delta propeller. This is but one part of the Theodorsen equation: the remaining part

agrees with the thrust component of the blade normal pressure, as evaluated in Ref. 14. Thus, Theodorsen's general equation in the limit $\lambda \to \infty$ agrees exactly term by term with Ribner's equation for the total thrust of the delta propeller. This result, so far as it goes, is supportive of the credibility of both analyses.

A final caveat: the results herein apply solely to single rotation propellers whose blades trace helicoidal paths; the hub is not allowed for as well. This excludes certain unusual shapes, such as those with winglet-like tip vanes.[19] It is intuitively evident that these vanes should constrain the fluid to reduce the spillage around the blade tips: the tip loss. Stated otherwise, the vanes will increase the thrust-effective cross-sectional area of the wake, and, hence, the values of κ and ϵ, at a given advance. The effects should be somewhat equivalent to an increase in the number of blades.

Acknowledgments

Support at the University of Toronto was aided by a grant to the first author from the Natural Sciences and Engineering Research Council of Canada, and by his tenure part time at NASA Langley Research Center as a Distinguished Research Associate. The computations were carried out on the Cray X-MP/24 operated by the Ontario Centre for Large Scale Computation at the University of Toronto.

References

[1]"Aerodynamics and Acoustics of Propellers," *Proceedings of AGARD Conference, No. 366,* Fluid Dynamics Symposium, Toronto, Canada, Oct. 1-4, 1984.

[2]Hanson, D. B., "Compressible Lifting Surface Theory for Propeller Performance Calculation," *Journal of Aircraft,* Vol. 22, Jan. 1985, pp. 19-27.

[3]Schone, J., "A Doublet Point Method for the Calculation of Unsteady Propeller Aerodynamics," *Notes on Numerical Fluid Mechanics,* Vieweg Verlag, Braunschweig, FRG, 1987.

[4]Theodorsen, T., "The Theory of Propellers. I—Determination of the Circulation Function and the Mass Coefficient for Dual-Rotating Propellers," NACA Rept. No. 775, 1944.

[5]Theodorsen, T., "The Theory of Propellers. II—Method for Calculating the Axial Interference Velocity," NACA Rept. No. 776, 1944.

[6]Theodorsen, T., "The Theory of Propellers. III—The Slipstream Contraction with Numerical Values for Two-Blade and Four-Blade Propellers," NACA Rept. No. 777, 1944.

[7]Theodorsen, T., "The Theory of Propellers. IV—Thrust, Energy, and Efficiency Formulas for Single- and Dual-Rotating Propellers with Ideal Circulation Distribution," NACA Rept. No. 778, 1944.

[8]Theodorsen, T., *Theory of Propellers,* McGraw-Hill, New York, 1948.

[9]Betz, A., "Screwpropeller With Least Energy Loss," *Göttinger Nachrichten,* in German, 1919, pp. 193-213; reprinted in *Vier Abhandlungen zur Hydrodynamik und Aerodynamik,* Göttingen, 1927, pp. 68-92.

[10]Goldstein, S., "On the Vortex Theory of Screw Propellers," *Proceedings of the Royal Society,* London, England, Vol. 123, 1929, pp. 440-465.

[11]Lock, C. N. H., and Yeatman, D., "Tables for Use in an Improved Method of Airscrew Strip Theory Calculation," R. & M. 1674, British Aeronautical Research Council, Oct. 1934.

[12]Kramer, K. N., "The Induced Efficiency of Optimum Propellers Having a Finite Number of Blades," in German, *Luftfahrtforschung,* Vol. 15, July 6, 1938, pp. 326-333, translated in NACA TM 884.

[13]Foster, S. P., "Ideal Efficiency of Propellers Based on Theodorsen's Theory: A Review and Computer Study with Extended Plus Simplified Charts," Univ. of Toronto Inst. for Aerospace Studies, Downsview, Ontario, Canada, UTIAS TN NO. 271 (to be published).

[14]Ribner, H. S., "A Transonic Propeller of Triangular Plan Form," NACA TN-1303, 1947.

[15]Ribner, H. S., "Damping in Roll of Cruciform and Some Related Delta Wings at Supersonic Speeds," NACA TN 2285, 1951.

[16]Westwater, F. L., "Some Applications of Conformal Transformations to Airscrew Theory," *Proceedings of Cambridge Philosophical Society,* Vol. 32, Pt. 4, Oct. 1936, pp. 676-684.

[17]Mikkelson, D. C., Mitchell, G. A., and Bober, L. J., "Summary of Recent NASA Propeller Research," NASA-TM 83733, 1984.

[18]Lock, C. N. H., "An Application of Prandtl Theory to an Airscrew," R. & M. 1521, British Aeronautical Research Council, i-v, 1-41, 12 figures.

[19]Sullivan, J. P., Chang, L. K., and Miller, C. J., "The Effect of Proplets and Bi-Blades on the Performance and Noise of Propellers," *Transactions of the Society of Automotive Engineers,* Vol. 90, No. 2, Dec. 1982, pp. 2106-2113.